Coastal new particle formation: Environmental conditions and aerosol physicochemical characteristics during nucleation bursts

Colin D. O'Dowd,[1,2,3] Kaarle Hämeri,[1] Jyrki Mäkelä,[1] Minna Väkeva,[1] Pasi Aalto,[1] Gerrit de Leeuw,[3,4] Gerard J. Kunz,[4] Edo Becker,[3,5] Hans-Christen Hansson,[6] Andrew G. Allen,[7] Roy M. Harrison,[7] Harald Berresheim,[8] Christoph Kleefeld,[2] Michael Geever,[2] S. Gerard Jennings,[2] and Markku Kulmala[1]

Received 28 November 2000; revised 15 June 2001; accepted 15 June 2001; published 11 September 2002.

[1] Nucleation mode aerosol was characterized during coastal nucleation events at Mace Head during intensive New Particle Formation and Fate in the Coastal Environment (PARFORCE) field campaigns in September 1998 and June 1999. Nucleation events were observed almost on a daily basis during the occurrence of low tide and solar irradiation. In September 1998, average nucleation mode particle concentrations were 8600 cm^{-3} during clean air events and 2200 cm^{-3} during polluted events. By comparison, during June 1999, mean nucleation mode concentrations were 27,000 cm^{-3} during clean events and 3350 cm^{-3} during polluted conditions. Peak concentrations often reached 500,000–1,000,000 cm^{-3} during the most intense events and the duration of the events ranged from 2 to 8 hours with a mean of 4.5 hours. Source rates for detectable particle sizes ($d > 3$ nm) were estimated to be between 10^4 and 10^6 cm^{-3} s^{-1} and initial growth rates of new particles were as high as 0.1–0.35 nm s^{-1} at the tidal source region. Recently formed 8 nm particles were subjected to hygroscopic growth and were found to have a growth factor of 1.0–1.1 for humidification at 90% relative humidity. The low growth factors implicate a condensable gas with very low solubility leading to detectable particle formation. It is not clear if this condensable gas also leads to homogeneous nucleation; however, measured sulphuric acid and ammonia concentration suggest that ternary nucleation of thermodynamically stable sulphate clusters is still likely to occur. In clear air, significant particle production (>10^5 cm^{-3}) was observed with sulphuric acid gas-phase concentration as low as 2×10^6 molecules cm^{-3} and under polluted conditions as high as 1.2×10^8 molecules cm^{-3}. *INDEX TERMS:* 0305 Atmospheric Composition and Structure: Aerosols and particles (0345, 4801); 0365 Atmospheric Composition and Structure: Troposphere—composition and chemistry; 0322 Atmospheric Composition and Structure: Constituent sources and sinks; *KEYWORDS:* aerosols, nucleation, tides, coastal particles

Citation: O'Dowd, C. D., et al., Coastal new particle formation: Environmental conditions and aerosol physicochemical characteristics during nucleation bursts, *J. Geophys. Res.*, *107*(D19), 8107, doi:10.1029/2000JD000206, 2002.

1. Introduction

[2] Along with understanding the direct interaction between aerosols and radiation and aerosols and clouds, understanding the formation and transformation of these aerosols is crucial to underpinning their relevance to processes leading to climate change. Considerable advances have been made in understanding the transformation and evolution of the aerosol size distribution through coagulation, condensation, aqueous phase chemical processes and deposition processes resulting in a reasonably accurate knowledge of primary influences which shape and evolve the distribution of atmospheric aerosols; however, significantly less progress has been made in our understanding of new particle formation in the unperturbed atmosphere.

[3] Understanding new particle formation has set forth demanding challenges to our physical and chemical technical ability along with our theoretical understanding. While

[1]Department of Physics, University of Helsinki, Helsinki, Finland.
[2]Department of Physics, National University of Ireland, Galway, Ireland.
[3]Centre for Marine and Atmospheric Sciences, University of Sunderland, Sunderland, UK.
[4]TNO Physics and Electronics Laboratory, The Hague, Netherlands.
[5]Now at Spectroscopic On-Line Analysis, Program Development, BP Chemicals Ltd., Hedon, UK.
[6]Institute for Applied Environmental Research, Air Pollution Laboratory, Stockholm, Sweden.
[7]Institute for Public Health, School of Chemistry, University of Birmingham, Edgebaston, Birmingham, UK.
[8]German Weather Service, Meteorological Observatory, Hohenpeissenberg, Germany.

0148-0227/02/2000JD000206$09.00

there have been a number of reports on new particle formation events in the natural unperturbed atmosphere [*Clarke et al.*, 1998; *Weber et al.*, 1998; *Covert et al.*, 1992; *O'Dowd et al.*, 1997a, 1997b; *Schröder and Ström*, 1997], there are few places that these events occur so frequently that one can accumulate a significant database on the range of environmental conditions under which nucleation occurs and consequently help us evaluate our current thinking on homogeneous nucleation of natural aerosol particles.

[4] Given that coastal nucleation occurs almost on a daily basis along the western coast of Europe [*O'Dowd et al.*, 1998], the Mace Head Atmospheric Monitoring Station was chosen as the location for the New Particle Formation and Fate in the Coastal Environment (PARFORCE) dedicated study into new particle formation processes. PARFORCE ran from January 1998 until January 2000 and comprised continuous long-term measurements of aerosol properties during coastal nucleation events along with two intensive field campaigns: the first during September 1998 and the second during June 1999 [*O'Dowd et al.*, 2002]. An airborne spatial mapping campaign also overlapped with the second intensive campaign [*O'Dowd*, 2002].

[5] The primary objectives of PARFORCE were to:

1. Determine the environmental conditions and the rates under which homogeneous heteromolecular nucleation occurs in the coastal boundary layer.
2. Examine whether these nucleation events can be explained by binary or ternary heteromolecular nucleation of: H_2SO_4-H_2O, NH_3-H_2SO_4-H_2O or NH_3-H_2O-MSA/HCl/HNO_3, or whether alternative nucleation schemes are likely to explain the observed events, i.e., organic embryo formation followed by organic and/or sulphate growth.
3. Examine the influence of anthropogenic/continental air parcel mixing on coastal nucleation.
4. Explore the growth rates of newly formed particles.
5. Examine the long-term frequency of occurrence of coastal nucleation bursts and their duration.

[6] This particular study primarily addresses objective 1 above and reports on the environmental conditions under which coastal nucleation occurs. Additionally, this study also contributes to meeting objective and 4 to examine the influence on anthropogenic/continental sources on coastal nucleation and to explore source and growth rates of new particles. An additional objective of this study is to document and characterize the physicochemical properties of new particles.

2. Instrumentation and Techniques

2.1. Aerosol Instrumentation

[7] Given the current technological limitation in aerosol instrumentation, it is not possible to measure actual new particles since these new particles are thought to occur at sizes of about 1 nm and typical particle spectrometers or total particle counters cannot effectively count or size particles below 3 nm. Hence we only measure recently formed particles after they have grown by coagulation and/or condensation processes. To measure particle concentration larger than 3 nm, a TSI 3025a condensation particle counter (CPC) was used. A modified TSI 3010 was used to measure particle concentration larger than 5 nm while a standard TSI 3010 was used to measure concentration larger than 10 nm [*Hämeri et al.*, 2002]. By taking the difference in measured concentration between the three CPCs in parallel, fast response measurements of nucleation mode particle concentration between 3, 5 and 10 nm were achieved.

[8] Previous results indicated that, while apparently ubiquitous along the coastline, the spatial scales of individual bursts were of the order of 10 to 100 m [*O'Dowd et al.*, 1998]. With that in mind, a pyramid-shape spatial array of CPCs was deployed during the first campaign with three nodes forming a near-surface level triangle and a fourth node operated at a height of 20 m. The near-surface level nodes were separated by approximately 150 and 200 m. The central node was located on a 10 m tower at the shore laboratory at Mace Head approximately 50–100 m from the tidal zone, while the elevated node at 20 m was also located beside the shore laboratory. Both these nodes (10 m and 20 m) comprised CPCs with cut-off sizes at 3, 5, and 10 nm. The third node was located 300 m inland (east) from the coastline while the fourth node was located on a small island adjacent to the coastline and north of the shore laboratories. This small island was separated from the mainland by water at high tide and connected to the mainland by the tidal zone during low tide. On the island node and the inland node, only one CPC, measuring concentrations >3 nm, was deployed elevated 2 m from the surface.

[9] All CPCs were logged centrally on one computer at a frequency of 10 Hz; however, later frequency analysis showed that the maximum reliable frequency that could be used was 1 Hz. [*Hämeri et al.*, 2002]. During the first campaign, particle concentrations were so large that the CPCs almost reached saturation and could not actually count true concentrations during the most intense events.

[10] The upper concentration limit achieved was 180,000 cm^{-3}; however, subsequent laboratory studies provided a coincidence correction factor and illustrated that, at saturation, true concentrations were likely to be six times higher than the raw-counts [*Hämeri et al.*, 2002]. In the second field campaign, the inland node was configured with a 30-times dilution system in an attempt to sample real concentration encountered in this environment. A detailed analysis of the CPC frequency response, cut-off sizes and concentration limitation can be found in [*Hämeri et al.*, 2002]. In this study, particle concentration measured by the CPCs was corrected for coincidence loss determined from laboratory experiments [*Hämeri et al.*, 2002].

[11] To provide aerosol size distribution measurements, a Differential Mobility Particle Sizer (DMPS), sampling from 3 to 500 nm over 10 min intervals was deployed in the shore lab attached to the community aerosol sampling duct [*Mäkelä et al.*, 1997]. Supermicron measurements over the size range from 0.5 to 300 μm were taken using Particle Measurement Systems Inc. (PMS) forward scattering spectrometer probe (FSSP) and a PMS optical array probe (OAP) optical particle counters. These particle counters sample wet-ambient size distributions while the submicron spectrometers sampled dry spectra.

[12] Total particle concentrations can be derived from the TSI 3025 CPCs or from the DMPS integrated concentration. In this environment, however, the concentrations are sometimes so high that the CPCs readily saturate (at 180,000

cm^{-3}) and thus only provide a lower estimate of the concentration. DMPS measurements are subject to significant losses in nucleation mode sizes that are not accurately characterized and thus total aerosol concentrations from the DMPS are also somewhat lower than anticipated actual concentrations. Probably the most accurate method for determining total particle concentration is from the diluted (thirty times) CPCs; however, since the diluted CPC was only available for 3 weeks during the second campaign, the DMPS concentration is taken as the standard. An evaluation of the different methods for measurements of high particle concentrations is presented in *Hämeri et al.* [2002].

[13] Growth factors, giving hygroscopic properties, of 8, 10 and 20 nm particles were taken using a Humidity Tandem DMPS (TDMA) [*Väkevä et al.*, 2002]. The TDMA is an instrument system that can be used to study hygroscopic growth processes leading to changes in particle size. This technique is well established and is nowadays a standard method for determining the hygroscopic growth factor of submicron particles and is extended in this study to cover nucleation mode or ultrafine (UF) mode particles. The growth factor is defined as the ratio between particle diameter at 90% relative humidity (RH) and dry conditions. The measurements were undertaken every 10 min, and thus the measurement cycle was half of an hour; i.e., each size was measured 2 times per hour. The UF-TDMA was placed in a mobile laboratory next to the shore laboratory and the sampling of air was done from the height of 10 m. TDMA measurements are described in more detail in *Väkevä et al.* [2002]. The growth factor for 8 nm ammonium sulphate particles is 1.4, while for 20 nm particles, it is 1.5. Aerosol mass and chemical composition were measured using filter packs and a Micro-Orifice Uniform Deposit Impactor (MOUDI) covering sizes from 0.062 to 20 μm.

2.2. Gas-Phase Measurements

[14] A range of gas-phase species, relevant to aerosol formation, was measured in parallel to the aerosol measurements. These covered species such as NH_3, SO_2 H_2SO_4, OH, methane sulphonic acid (MSA), O_3, IO, VOCs (C_8-C_{16}) and various halocarbons). SO_2 was measured with a Parallel Plate Denuder (PPD) while ammonia was measured with a diffusion scrubber with water as the absorbent. H_2SO_4, OH and MSA were measured using a chemical ionization mass spectrometer (CIMS) [*Berresheim et al.*, 2002]. Adjunct measurements of IO were taken for a limited period using a long path differential optical absorption spectroscopy (LP-DOAS) and are discussed by *Alicke et al.* [1999]. Similarly, halocarbons (CH_3Br, CH_3I, CH_2ClI CH_2I_2, $CHBr_2I$) were also measured for a limited period in the shore laboratory using mass spectrometry techniques and are discussed in [*Carpenter et al.*, 1999; *Carpenter and Liss*, 2000]. C_8-C_{16} volatile organic compounds were measured also using GC-FID and GC-MS [*Sartin et al.*, 2002]. Hydrogen peroxide and organic peroxides were also measured using HPLC techniques [*Morgan and Stroh*, 2002].

2.3. Meteorological Measurements

[15] Standard meteorological measurements (wind speed, wind direction, relative humidity, air temperature, solar radiation (total and ultraviolet) were available as standard parameters at Mace Head. In addition to these standard measurements, micrometeorological measurements were also conducted at the shore lab from 3 and 20 m. The micrometeorological measurements comprised fast response (3-D) wind field and temperature measurements using a Gill Ultra-Sonic anemometer while water vapor fluxes were determined with a Licor IR absorption device. From this package, vertical fluxes of heat, water vapor and momentum were acquired along with drag co-efficient and wind stress. Additionally, gradient measurements of 3-D wind fields and momentum fluxes, stress and drag coefficients were also taken at 5, 10, 15 and 20 m using a tri-axes Gill propeller anemometer system. A detailed characterization of the local micrometeorology and fluxes is given by *de Leeuw et al.* [2002]. Boundary layer structure was determined using a LIDAR (Light Detection And Ranging) system and by in situ measurements using an aircraft. A full report on boundary layer structure measurements is given in *Kunz et al.* [2002]. $JO(^1D)$ measurements were also taken using a high-resolution filtered radiometer to provide a measure of photochemical activity. Tide amplitude was calculated using a standard tide prediction software package for the area and during the second (June) campaign; water column pressure was measured to give tide amplitude variation.

3. Results

3.1. Particle Concentration and Low Tide Occurrence

[16] Nucleation bursts were observed almost on a daily basis throughout the whole PARFORCE program and, consistent with initial studies of coastal nucleation by *O'Dowd et al.* [1998, 1999b], were found to occur coinciding with low tide occurrence in the presence of solar radiation. The link between nucleation events and low-tide occurrence is best illustrated through examination of a relatively long time series of total aerosol concentration ($d > 3$ nm) over a period of ≈3 months. Figure 1 displays a surface contour plot of total aerosol concentrations and low-tide occurrence (marked by +). A clear pattern of elevated total aerosol concentrations is visible when low tide occurs during daylight hours. The tracking of the peak in total aerosol concentrations follows closely that of daytime low tide occurrence.

[17] Two intensive, four-week, PARFORCE field campaigns were conducted: one in September 1998 and another in June 1999. During both field campaigns, particle production was similarly observed to track low tide occurrence and was observed on approximately 90% of the measurement days, regardless of clean, moderately polluted or very polluted air masses. An example of total particle concentration during tidal-related nucleation bursts, observed during the second campaign in 1999, is shown in Figure 2 along with the tidal amplitude variation, sulphuric acid concentration and $JO(^1D)$. Typically, one event was observed on a nucleation day; however, on this day, owing to the timing of low tide, two tidal events occur during daylight hours, one in the early morning at JD 171.2 and another in the evening at JD 171.7. These two daylight low tide occurrences resulted in two nucleation events. During the first event, background total particle concentrations ($d >$ 3 nm) increased from ≈500 cm^{-3} to almost 30,000 cm^{-3}, while during the later event, concentrations increased to a peak of more than 40,000 cm^{-3} and lasted for ≈6 hours.

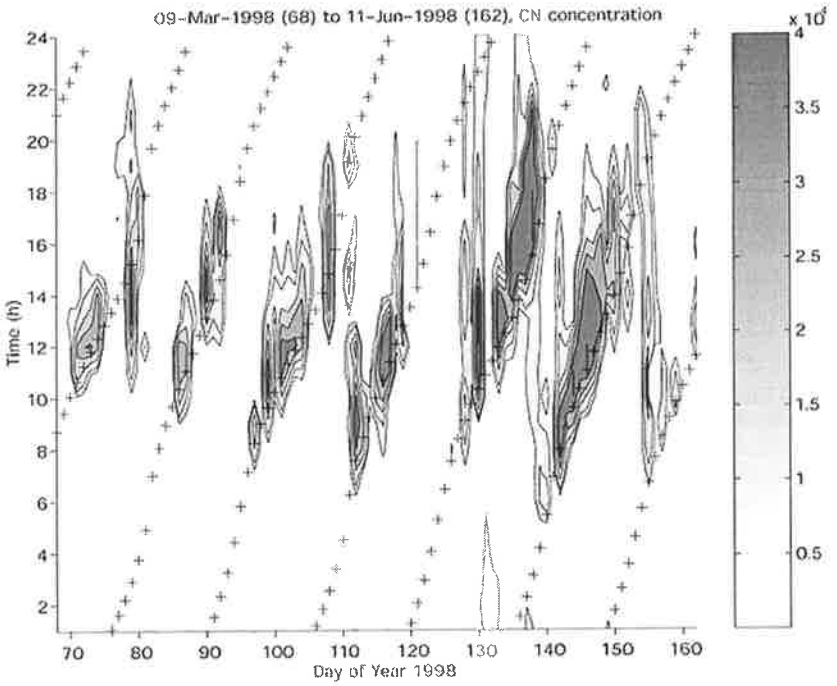

Figure 1. Contour plot of total (1-hour average) particle concentration, time of day and low tide occurrence (marked by +). Color bar scale units are particles cm^{-3}.

The morning event was somewhat shorter in duration (3 hours) and occurred about 1 hour after the lowest watermark, and appeared to start just at dawn. From the $JO(^1D)$ signal, it appears that, if one of the influencing processes is photochemically driven, a very small amount of radiation is required to promote nucleation. Particle nucleation starts to occur as the production rate of $O(^1D)$ increases from nighttime level of zero to 1×10^{-7} s^{-1}. The peak photolysis rate, on this day, was 2.5×10^{-5} s^{-1} and occurred almost exactly at midday. The formation of new particles under very low light levels at dawn was also observed previously at Mace Head during the ACSOE/MAGE field campaigns [see, e.g., *O'Dowd et al.*, 1998]. Also shown in this figure is the concentration of sulphuric acid, although no data are available for the dawn event. Peak sulphuric acid concentrations of 1.5×10^7 molecules cm^{-3} occur in the late afternoon, but significantly before the evening nucleation event. Sulphuric acid concentrations during this evening burst are of the order of $2-3 \times 10^6$ molecules cm^{-3}.

[18] Nucleation mode particle concentrations (3–20 nm) derived from DMPS measurements, along with tidal height variation, throughout the two intensive field campaigns are shown in Figure 3. During the September campaign (Julian day (JD) 250–275, 1998) regular peaks in particle concen-

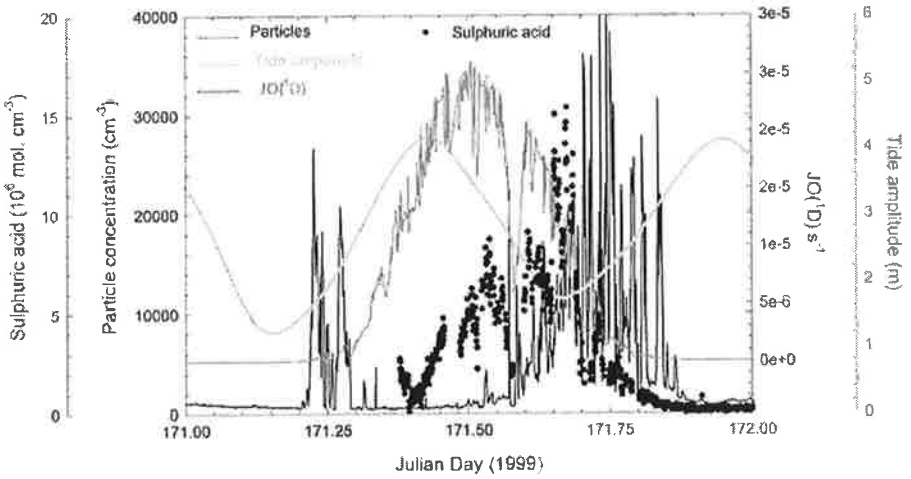

Figure 2. Total particle concentration (d > 3 nm), $JO(^1D)$, sulphuric acid, and tidal amplitude during two coastal particle production events, June 1999.

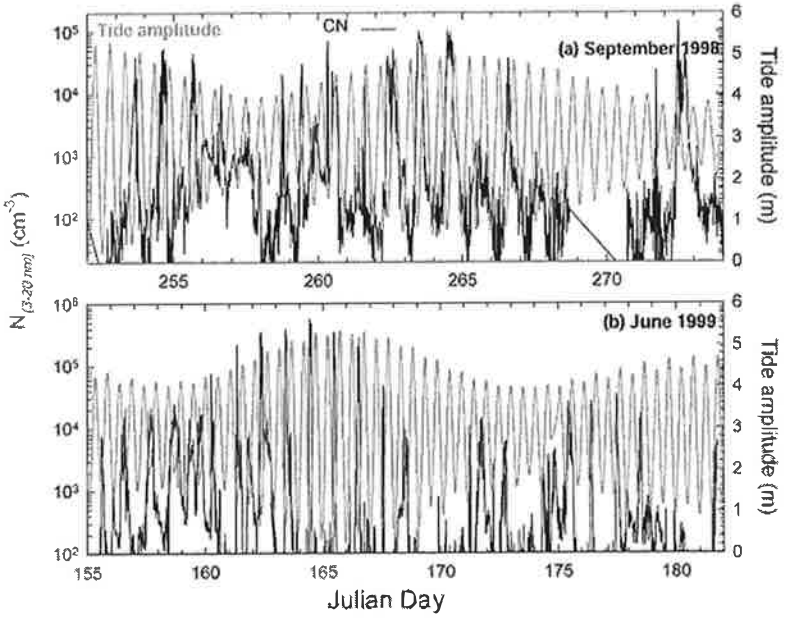

Figure 3. (a) Ultrafine (3–20 nm) particle concentration during the first PARFORCE intensive field campaign in September 1998; (b) total particle concentration and tidal amplitude during the second PARFORCE intensive campaign in June 1999. Tide height in meters is given on the right-hand side axis.

tration can be seen almost every day. Nucleation mode particle concentration reached $>10^5$ cm^{-3} during the most intense events over this period. A similar pattern is seen during the second campaign (JD 155–182), where peaks in nucleation mode particle concentration are seen, again, almost daily. The occurrence of elevated nucleation mode particle peaks is clearly illustrated for both periods where all the nucleation mode peaks are observed to occur during low-tide conditions under daylight hours. During this second campaign, a series of very intense events occur 6 days in a row (JD 161–166) and a peak concentration of almost 6×10^5 cm^{-3} is observed on JD 164. It should be noted that the DMPS concentrations are derived from 10 min size distributions and, as a result of this slow time resolution, it does not capture higher peak concentrations over shorter timescales. For this particular case, the total particle concentration measured by the CPCs indicated a particle concentration peaking at 1.2×10^6 cm^{-3} over shorter timescales.

[19] It appears the more intense events occurred during the June campaign compared to the September campaign. This is confirmed by a statistical analysis of the mean nucleation mode particle concentration during both campaigns. In doing this analysis, events occurring in clean air were classified on the basis of preexisting particle concentration (>20 nm) being less than 1300 cm^{-3}, while events with preexisting concentration greater than this value were classified as polluted events, in conjunction with other traces. For the September campaign, the mean clean preexisting aerosol concentration was 235 cm^{-3}, while the mean nucleation mode particle concentration was 8600 cm^{-3}. Under polluted conditions, the mean preexisting aerosol concentration was 6500 cm^{-3} while the mean nucleation mode particle concentration was 2200 cm^{-3}. By comparison, during June, the mean clean nucleation mode concentration was 27,000 cm^{-3} and the preexisting concentration was 550 cm^{-3}. For polluted conditions during June, nucleation mode concentrations were 7900 cm^{-3} compared to a background concentration of 3350 cm^{-3}. These mean

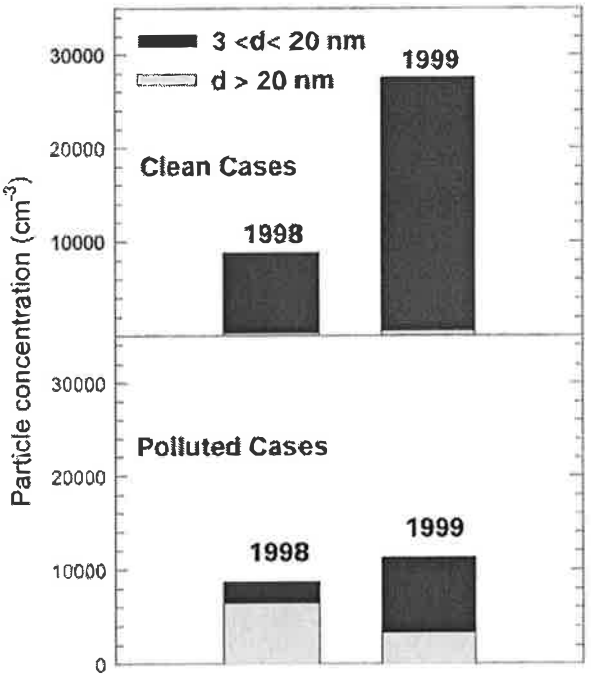

Figure 4. Mean ultrafine (3–20 nm) and preexisting (>20 nm) particle concentration during the 1998 and 1999 intensive PARFORCE field campaigns for clean and polluted air masses.

Table 1a. Environmental Conditions for Nucleation Bursts and Type Classification for the 1998 Intensive Field Campaign[a]

JD	Type	SO_2, ppt	NH_3, ppt	Soot, ng m^{-3}	Wind Speed, m s^{-1}	Wind Direction, degrees	T, °C	RH, %
250	II[b]			5–25				86–99
251	I			30–50	10–15	200	16–18.7	96–99
252	I		50–100	0–15	8–11	260–280	16–18.2	86–98
253	II		20–80	7–32	8–18	290–320	13–14	70–95
254	II		500–1700	6–36	10–14	300–240	12.5–15.5	60–92
255	II	10–20	1500–1700	5–25	12–18	300	12–14.5	70–92
256	II	<10	800–500	5–15	7–12	325	13–16	84–94
257	I[b]	20–70	50–70	10–20	8–10	240–260	13–14	78–82
258	II	10–30?		10–15	5–8	300–320	13.5–14.5	85–95
259	II	20–40	20–25	5–10	3–5	280–320	14–15	95–99
260	III[b]	500–1000	20–150	150–250	5–7	100–120	13–15	95–100
261	I	35–60	100–150	5–30	5–8	190–220	17–18.5	92–98
262	III	100–5000	40–180	100–250	3–6	120–180	15.5–19	83–98
263	III	1000–7000	500–2000	600–800	6–8	110–140	18–23	85–90
264	III	1–10 ppb	400–1700	700–800	4–7	110–140	20–24	65–88
265	IV[b]	1.1 ppb	500–750	700–800	4–5	110–140	22–24	65–70
266	III	0.5–1 ppb	500–1200	850–1300	3–7	80–120	14–18	
267	no event	1 ppb	1000–2000	1350–1600	3–6	60–100	13–16.5	70–100
268	I	1–1.2 ppb	600		6–8	70–90	16–17	97–99
269	IV	1–3 ppb	800–1100		3–6	30–60		
270	IV		300–600	600–1000	6–9	330	15–16	90–95
271	I	20	750	100–350	6–9	190–230	15.5–17	80–85

[a]Blank values are where data were not available.
[b]No burst or otherwise unclassified event.

statistics are graphically illustrated in Figure 4. Clearly, the nucleation mode concentration during the Summer campaign are, on average, three times greater than that occurring in Autumn campaign, regardless of clean or polluted air masses. This higher average nucleation mode concentration during bursts in summer may be due to enhanced biological emission and photochemical activity during summer compared to autumn. While there is no data to corroborate enhanced biological activity, the $JO(^1D)$ measurements indicate peak production rates of 1.8×10^{-5} s^{-1} in September compared to 2.6×10^{-5} s^{-1} in June (i.e., >30% higher in June); however, it should be noted that during the most intense particle period in June (JD 161–166) the $O(^1D)$ source rates are no higher than on other, less productive, days. The events were classified into four categories: types I, II, III, IV, and this classification is

Table 1b. Environmental Conditions for Nucleation Bursts and Type Classification for the 1999 Intensive Field Campaign[a]

JD	Type	SO_2, ppt	NH_3, ppt	Soot, ng m^{-3}	Acid, 10^6 cm^{-3}	Wind Speed, m s^{-1}	Wind Direction, degrees	T, °C	RH, %
156	II			20	10–15				
157	II	60		50	10–15	4–5	270	12	55–60
158	II	120	25–50	20	10–15	4–5	270	12	55–60
159[b]	unclassified	50–100	50–400	50–400	5	4–5	270–300	13–14	60–70
160	II	20–50	20–50	20	4	1–3	270–300	10–11	80
161	II	10–30	10	20	4	2–3	270–300	12	80
162	II, II	50	125	150	1.5–2	3	180–270	10–12	80
163	II	20–30	25	30	2	4	300	10–11	70–80
164	I	20–90	20	20	6–8	3–5	200	12–14	85–95
165	I	60	25	20	8–12	4	200	13–14	85–95
166[b]	II[c]	2600–150	50–100	300–50	5(12)	6–8	90–180	12–14	85–95
167	I	20–30	50–125	20–30	4	6–7	200–230	13	90–95
168	unclassified	150	50–70	30	13	4	240	12–13	70–80
169	I	40	0	30		5–6	180–200	13–14	95
170	no burst	0–15	X	10–20		10–12	200–250	13–14	90–95
171	I, II?	5, 200–50	50	10–20	5–15	5–6	270	11–13	70–75
172	I, U	10,60	35	10–20	4–8	3–4	180–270	12	60–70
173[b]	no burst	0–20	<50	0–20	0	4–6	200–270	12	80–90
174	I, I	50–1000	1000, n/a	10, 40	3	1–4	220–280	13	70–80
175	III	2000	900	>1000	30–120	1–3	90–270	15–16	70–80
176	III	2500	1300	>1000	60–80	2–4	90–180	14–15	70–85
177	I		<50			4–8	180–270	11–13	80–95
178[b]	I[c]		<100	20	10–15	5–6	250–270	11–13	70–80

[a]Blank values are where data were not available.
[b]No burst or otherwise unclassified event.
[c]Possible local pollution or unclear.

Table 2a. Total Aerosol Chemical Composition During the 1998 Intensive Field Campaign

JD	Type	nssS, ng m^{-3}	Cl^-	NH_4^+
250	II			
251	I			
252	I	860	6320	20
253	II	750–960	5950–6320	20–50
254	II	770–820	4240–5900	30–100
255	II	650–960	5860–7000	0–20
256	II	420–450	3040–4060	0–20
257	I	420–1180	4060–7420	20–30
258	II	790–870	4460–5680	0–60
259	II	790–1290	3570–4460	60–170
260	III	1130	3570	170
261	I	1190–2230	14580–16570	10–270
262	III	440–2510	4080–7760	130–480
263	III	5530–8300	540–5920	1350–2160
264	III	7760–8500	110–1390	1810–2270
265	IV	13000–13130	180–290	4110–6710
266	III	11320–13230	150–400	4020–4740
267		11231–15220	280–650	4290–6250
268	I	17560–20190	770–1060	7010–8690
269	IV	14900–17150	360–610	5050–8270
270	IV	5270–10270	360–690	1240–2230
271	I	800–2890	580–3910	260–700

discussed in detail later; however, to provide a brief definition for the moment, types I and II occurred in clean marine air; type III occurred in polluted or modified marine air and type IIII was a null event.

3.2. Range of Conditions

3.2.1. Meteorological and Gas-Phase Concentrations

[20] For the intensive campaigns, the basic meteorological conditions under which nucleation occurs, along with air quality tracers such as SO_2, ammonia and soot carbon are tabulated in Tables 1a and 1b. For the second field campaign, gas-phase sulphuric acid is also tabulated. Since events often lasted several hours, as seen in Figure 2, and the concentration of gas-phase parameters often vary significantly during the event periods, a statistical average is not conducted; however, the range of concentrations encountered for the duration of the event is reported instead. The events are defined as periods in which nucleation mode particle concentration is greater than 200 cm^{-3}.

[21] In terms of meteorological conditions, nucleation was observed to occur under wind speeds ranging from 1 to 18 m s^{-1}, temperatures ranging from 11°C to 24°C, and relative humidities ranging from 55 to 99%. In terms of air mass tracers, soot carbon is well characterized as a tracer over this region over the north Atlantic by *O'Dowd et al.* [1993] and at Mace Head, where soot loadings of less than 50 ng m^{-3} indicated the cleanest air masses, while soot concentrations of 100–300 ng m^{-3} indicated modified maritime, or moderately polluted air, and concentrations approaching or in excess of 1000 ng m^{-3} is typical of polluted air. From Tables 1a and 1b, it can be seen that nucleation occurs in the cleanest air masses with peak soot concentrations observed being of the order of 2–15 ng m^{-3} as well as under conditions where concentrations reached 1300 ng m^{-3}. No sulphuric acid concentrations were available during the 1998 campaign, but SO_2 is regarded as a surrogate for likely sulphuric acid concentrations. During this campaign, nucleation was observed for SO_2 concentrations as low as 10 ppt and as high as 10 ppb, although the latter cannot be regarded as natural SO_2 concentrations. Ammonia, implicated as a possible participant in nucleation [*Korhonen et al.*, 1999], was observed to range from 10 to 2000 ppt during events. For sulphuric acid, nucleation was observed to occur for concentrations ranging from between 2×10^6 molecules cm^{-3} and 1.2×10^8 molecules cm^{-3} under the most polluted conditions. In terms of event duration, typically an event lasted 3–6 hours, with peak durations of almost 8 hours being observed during spring tides for clean air. The mean duration of the events was 4.3 hours with a standard deviation of 2.4 hours. When tidal amplitude is high, the event duration tended to be longer than that occurring under minimal tidal amplitude since the fraction of exposed tidal regions is greater. Although the correlation coefficient between tidal amplitude and event duration was low ($r^2 = 0.26$), in general, the greater the tide amplitude, the longer the duration of the event.

3.2.2. Aerosol Chemical Composition

[22] Under clean conditions concentrations of aerosol excess (non-sea-salt) sulphate were typically <1.0 μg m^{-3}, with levels occasionally exceeding 20 μg m^{-3} in continental air masses. Aerosols within polluted air masses were neutralized to a greater extent than those present in clean Atlantic air, with associated median $[NH_4^+]$ / $[nssSO_4^{2-}]$ molar ratios for all particles of 1.91 and 0.24, respectively, corresponding to days 263–270 and 252–261 (1998). In fine particles (<2.5 μm diameter) ratios were 1.91 (polluted) and 0.58 (clean), showing that significant acidity was associated with the larger particles. During the 1999 campaign ammonium measurements were only available for the fine fraction, and ratios were more consistent throughout this period of mainly lightly modified marine air masses, with median values in the range 1.70–2.34.

[23] Concentrations of excess sulphate, chloride and ammonium during nucleation events are listed in Tables 2a and 2b. Chloride concentrations, used as an indicator for the

Table 2b. Total Aerosol Chemical Composition During the 1999 Intensive Field Campaign

JD	Type	nssS, ng m^{-3}	Cl^-	NH_4^{+a}
156	II			
157	II	190–380	3300–6300	170–220
158	II	180–420	2640–3800	180–220
159	unclassified	740–870	420–800	220–230
160	II	440–1180	920–13010	100–210
161	II	470–790	1730–10050	140–210
162	II	950–1220	1040–1290	320–330
163	II	760–850	2880–31310	110–240
164	I	850–2110	6430–20200	290–350
165	I	380–610	12480–17350	30–80
166	II	1470–2140	1280–13010	410–640
167	I	680	13360	150
168	U	250–370	11240–24310	80–150
169	I	1410–1890	7170–8970	160–340
170		610–700	16680–33190	80–220
171	I, II	50–350	12910–26830	0–50
172	I, unclassified	160–510	9710–23850	60–100
173		140–390	3290–23720	70–100
174	I	420–940	7000–21500	80–420
175	III	830–2410	620–2090	430–1190
176	III	2860–3680	1310–1590	1430–1660
177	I	480–1360	9470–31900	40–440
178	I	50–190	13000–24440	30–60

[a] Fine fraction only.

sea salt component of the aerosol, were seldom higher than 1.0 μg m^{-3} in the most polluted air masses (days 263–270, 1998) but frequently exceeded 20 μg m^{-3} at other times in maritime air. Coarse (>2.5 μm diameter particles) chloride levels were associated with sea spray generation, increasing with wind speed or when air traversed the coastline or offshore islands. Levels of fine particle chloride (up to around 0.7 μg m^{-3}) were also dependent on wind speed (in maritime air), with the contribution from the coastal region seen in a progressive rise in chloride levels on occasions when winds moved from southwesterly to southeasterly, traversing the coastal strip. Nitrate concentrations were <0.06 μg m^{-3} in clean air masses and increased to maxima around 10 μg m^{-3} in polluted air. A more rapid decline of nitrate concentrations relative to sulphate during periods of transition from more polluted to less polluted conditions indicated a longer atmospheric lifetime for sulphate than nitrate.

[24] Fine fraction non-sea salt sulphate concentrations in clean marine air varied in the range 0.1–0.4 μg m^{-3}, reaching a maximum of 17 μg m^{-3} in polluted easterly air masses. These data show that for 1998 unpolluted air was only present at Mace Head prior to JD260, and that continental aerosol contributed to excess sulphate on all other days. Similarly background ammonium concentrations were 0–0.05 μg m^{-3} in clean air and reached 9 μg m^{-3} in polluted air masses. Small increases in non-sea salt sulphate concentrations sometimes occurred near midday, probably as a result of diurnal shifts in rates of gas-phase oxidation (of DMS and/or SO_2). During 1999 concentrations of excess sulphate, as well as of nitrate, were on most days representative of marine air masses having a minor continental component, with North Atlantic background levels only measured during JD171-173 and JD178-179.

[25] MSA concentrations rarely exceeded 0.03 μg m^{-3} in clean air, but increased in NO_x-enriched polluted air masses, possibly as a result of enhanced rates of DMS oxidation. *Berresheim et al.* [2002] suggested that the MSA aerosol partitioning was very sensitive to relative humidity with large anti-correlations found between gas-phase MSA and dew point.

[26] There is insufficient data to include halocarbons and IO measurements in this analysis, while VOCs are omitted because no compounds with an aerosol formation potential were identified [*Sartin et al.*, 2002; *Mäkelä et al.*, 2002] and are not considered to be involved in this processes at Mace Head, although we cannot totally rule out the possibility that VOCs are involved in the aerosol formation processes. The possible role of halocarbons will, however, be discussed later.

3.3. Classification of Nucleation Event Types

3.3.1. Coastal Features Around Mace Head

[27] The coastal zone around the west coast of Ireland is quite inhomogeneous (see Figure 5a) with Mace Head located on a peninsula almost totally surrounded by coastline, and consequently, tidal zones. The location of the monitoring station and the peninsula nature of Mace Head itself provides a unique opportunity to study particle formation events at different distances from the tidal source region. Figure 5b displays four primary air trajectory regimes, each corresponding to different distances from the tidal source region. Type I air trajectories corresponds to clean marine airflow from the south to northwest sector in which the only tidal region encountered is that approximately 100 m from the measurements station. Type II also corresponds to clean marine air but with advection briefly over sparsely population land in the northwest-to-north sector. Airflow under this regime advects over multiple tidal zones 10–20 km upwind of the monitoring station along with the local tidal zone right at Mace Head. Type III conditions correspond to polluted air from the east to southerly sector and advecting over a tidal region 2–3 km from the station. Type IV conditions correspond to polluted air trajectories with no advection of tidal regions.

3.3.2. Nucleation Mode Particle Concentration

[28] While the local trajectory and event type classification is based on a combination of large scale air mass trajectory classification, number of tidal regions encountered and distance of measurement location from tidal region, measurements of nucleation events using CPC, DMPS and TDMA data were also similarly and consistently classified into four event types also. There were, however, some cases that were unclear and thus were not classified. Agreement of both methods resulted in a type being positively identified. Based on results from the first field campaign in 1999, the primary features associated with type I events were enhancement of particle concentration in the 3–10 nm size range and little or no growth into sizes larger than 10 nm. Peak particle concentrations during these events types ranged between 10,000 and 100,000 cm^{-3} and were typically lower than those encountered under other sectors. For wind speeds ranging from 5 to 20 m s^{-1}, the measurements correspond to point-measurements from between 5 and 20 s into the coastal plume. It should be noted that some of the strongest type I events resulted in particle concentrations as high as 10^6 cm^{-3}. By comparison, in a type II event, peak concentrations regularly reached in excess of 10^5–10^6 cm^{-3} and considerable growth into sizes larger than 10 nm was observed with as much as 50,000–100,000 cm^{-3} growing into this size range. For these event types, measurements correspond to point measurements approximately 30 min into the coastal plume evolution, with an additional plume from the local tidal region. For type III events, due to the fact that the air trajectories did not advect over a very local (i.e., 100 m) tidal zone, most of the new particles had grown to sizes larger than 5 nm by the time they were sampled at the monitoring station. Type IV events can be viewed as null events since the air mass trajectory does not advect over any tidal regions upwind of the monitoring station and no new particles are observed. From each of the two intensive field campaigns, two cases of types I, II, and III were selected for detailed process-study analysis in associated studies and are presented and their general features are discussed in the following sections.

[29] Figure 6 illustrates two cases each for types I, II, and III. For type I, JD 271 1998 and JD 165 1999 are taken as typical of these types of events. The general features associated with type I events is that noticeable enhancement is observed in 3 nm particle concentration but little or no enhancement is observed at sizes of 10 nm, presumably due

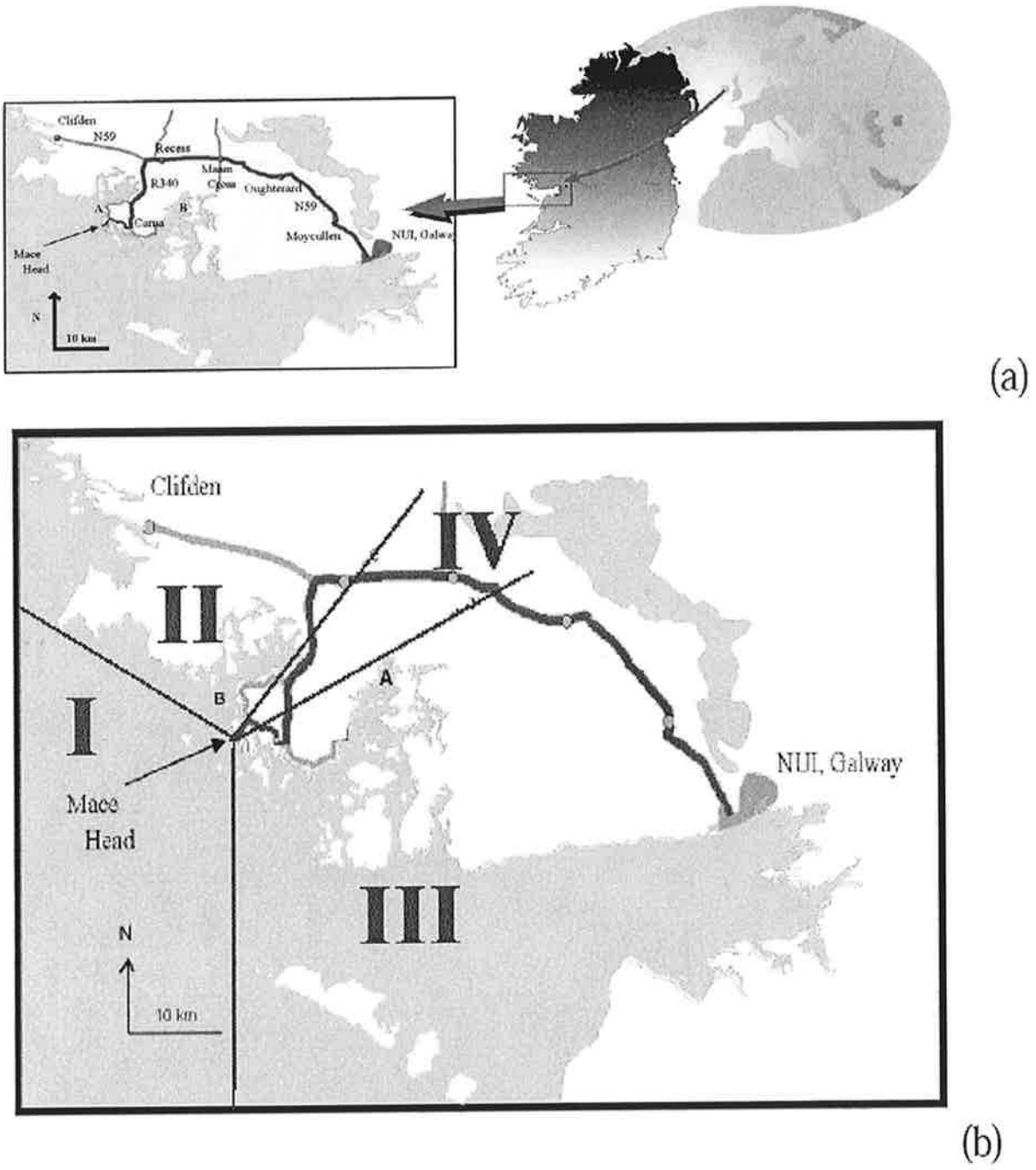

Figure 5. (a) Location of, and coastal features around, the Mace Head station and the West of Ireland; (b) local trajectory classification.

to the very short transit times from the production region and the measurement point. On JD 171, peak concentrations observed are of the order of 80,000–140,000 cm^{-3} and no enhancement is observed in particle concentrations at sizes larger than 10nm. For JD 165, peak concentrations approach 1,200,000 cm^{-3}, with a small enhancement in particle concentration at sizes larger than 10 nm (about 5000 cm^{-3}).

[30] Type II (JD 255, 1998, and JD 263, 1999) events generally indicated significant growth into 10 nm sizes some time after the first appearance of 3 nm particles and generally represents a signal characteristic of the air trajectory passing over 2 exposure zones, one about 10–20 km up-wind to the north-northwest, and the second zone being the local zone around Mace Head. On JD 255, 3nm particle

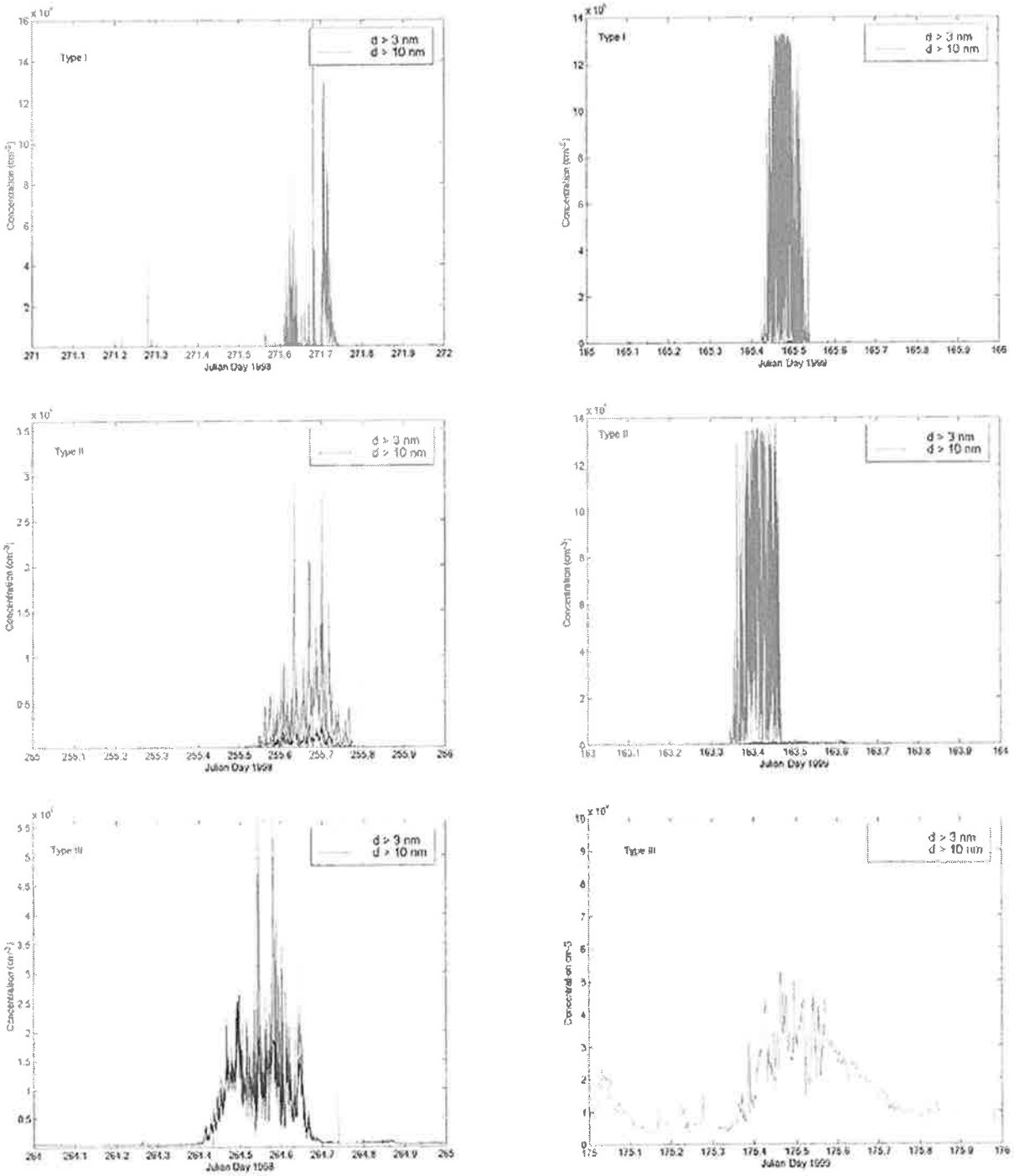

Figure 6. Typical examples of type I, II and III nucleation events as observed from the 10 m tower located beside the shore lab at Mace Head, approximately 100 m from the tidal region. Total concentration larger than 3 nm (rlight) and 10 nm (dark) are illustrated for each event type.

concentration increases to 150,000–300,000 cm^{-3} while on JD 163, concentrations reached >1 200 000 cm^{-3}. It should be noted that on JD 255, high winds and high humidity resulted in a significant enhancement to the aerosol condensation sink, possibly reducing the yield of new particles relative to JD 163. Type III events occur in polluted air (JD 264 1998 and 175, 1999) and can range from moderate events with particle concentration of the order of 50,000

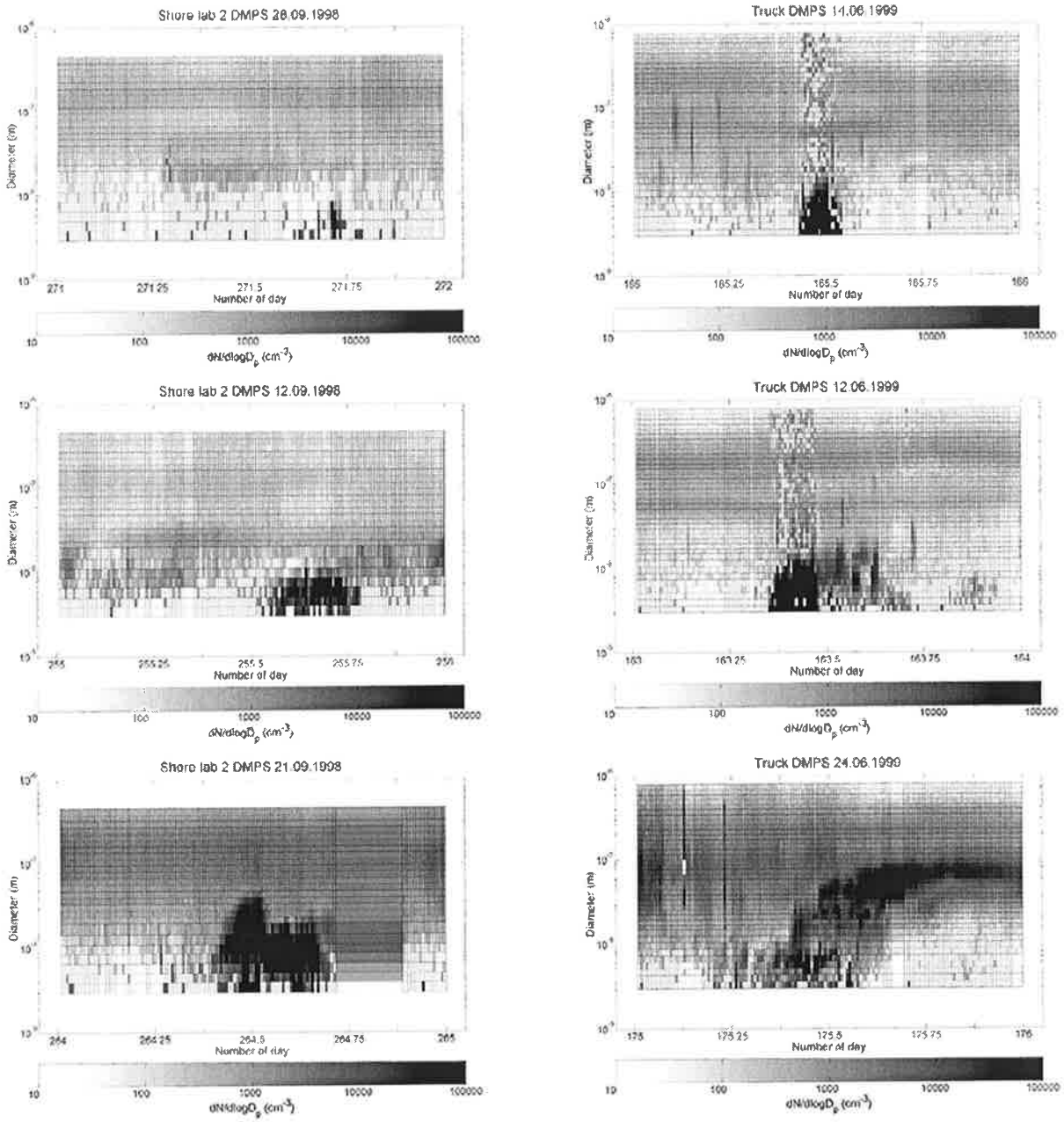

Figure 7. Size distributions of nucleation, fine and accumulation mode aerosol for event types I (top), II (middle), and III (bottom) during the 1998 (left column) and 1999 (right column) intensive field campaign.

cm^{-3}, or strong events with concentrations exceeding 220,000 cm^{-3}.

3.4. Submicron Size Distribution Measurements

[31] DMPS particle size spectrometry was used to determine submicron particle size distribution at 10 min timescales. As an output, number size distribution of the particles in the size range of 3–800 nm in diameter was obtained. The DMPS data of six characteristic days are shown in Figure 7 as color plots with time, as day of year, in the abscissa and particle diameter in the ordinate. The scaling shows the concentration of particles at each size class (in dN/dlogDp). The nucleation burst is shown in the middle of the day at the size range of particle diameter (Dp) below 20–30 nm. The left column of figures represents data from the September PARFORCE campaign and the right column, the June campaign. The upper plots are type I events, middle ones type II, and the lowermost are type III events.

[32] It is seen that in type I cases, the highest concentrations are found at the size below 5 nm, whereas in type II cases, the maximum concentration peak lies at 6–8 nm. The typical bimodal maritime background distribution is best seen in Figure 7. In type III cases the particle growth arising from below 10 nm to sizes above 20 nm is observed. The

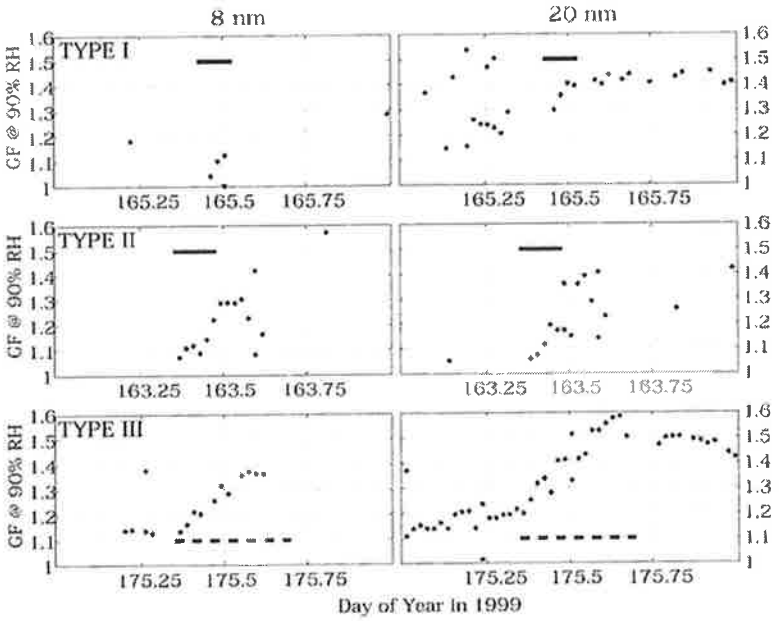

Figure 8. Growth factors for 8 nm and 20 nm particles during type I, II and III events days of June 1999. The duration of the nucleation event is highlighted by the solid bar for type I and II evens, while the nucleation and associated growth events in type III are highlighted by the dashed bar.

continental background particles at size range of 80–200 nm are also seen in the type III cases (Figure 7).

3.5. Nucleation Mode Particle Growth Factors

[33] Hygroscopic growth factor data are shown in Figure 8 for type I (165), type II (163) and type III (175) cases. During the type I days, the mode of the recently formed particles seldom reached 10 nm. Comparison of 8 nm and 20 nm growth factor data (see Figure 8) show that the preexisting (20 nm) particles have a different composition than the newly formed ones. Growth factors for 8 nm particles are typically 1–1.1, indicating a solubility significantly less than that of ammonium sulphate (1.4). Larger 20 nm particles typically have a growth factor of 1.5, but sometimes can be slightly lower at 1.3. Low growth factors of 8 nm particles indicate that they consist of insoluble organic or other weakly soluble inorganic species, possibly accompanied by a small soluble part. Simultaneous observations of 20 nm particles, on the other hand, reveal significant soluble fractions. DMPS measurements on the same day (JD 165) show that there is a change in size distribution of the preexisting particles prior to the observations of nucleation mode particles. An indication of a change can also be seen with TDMA. The externally mixed low solubility 20 nm particles seen during the night and early morning are replaced by internally mixed hygroscopic particles.

[34] During the type II days, 8 nm (and also 10 nm) growth factors first show similar characteristics (low growth factor) as on type I days, but later on in the day, they become more soluble. On the example day in Figure 8, 20 nm growth factors resemble those of 8 nm. During this particular day, and several other type II days, the 20 nm particles seem to be connected to the recently formed particles rather than to the larger preexisting ones. The 8 nm growth factors changed abruptly just before noon: first growth factors of the order 1.1–1.15 were seen resembling type I days, then about 1.3. This behavior might be explained by two different source regions of particles affecting the air mass along its history, or by chemical transformation of particles themselves or the condensing species they encounter while transported from further regions. Of course also a strong local source of a highly condensable gas might explain the rapid changes. During the campaign, sulphuric acid concentrations typically followed the solar radiation trend with peak concentrations occurring around noon [*Berresheim et al.*, 2002, Figure 12]. Generally, higher growth factors are observed in 8 nm particles around the peak sulphuric acid production period, suggesting that the increase in solubility may result from sulphuric acid condensation.

[35] Type III days resemble nucleation events observed at continental sites. Also here, however, low growth factors of both 8 and 20 nm particles are seen first, but later during the day growth factors become higher. This increase in growth factor again indicates the presence of a highly soluble condensing vapor. The measurements of growth factors of newly formed particles clearly indicated that sulphuric acid or ammonium sulphate are not the primary condensable species found on these new particles. These measurements point to a significant source of a weakly soluble inorganic or organic aerosol composition.

3.6. Source Rates and Growth Rates

[36] Although the CPC measurements were conducted at a temporal frequency of 10 Hz, subsequent frequency analysis determined that the highest usable frequency from these measurements was 1Hz [*Hämeri et al.*, 2002]. Nevertheless, this frequency is sufficient to allow determination of particle production rate, particularly for type I events. Considering that the source of particles in type I events is the tidal region

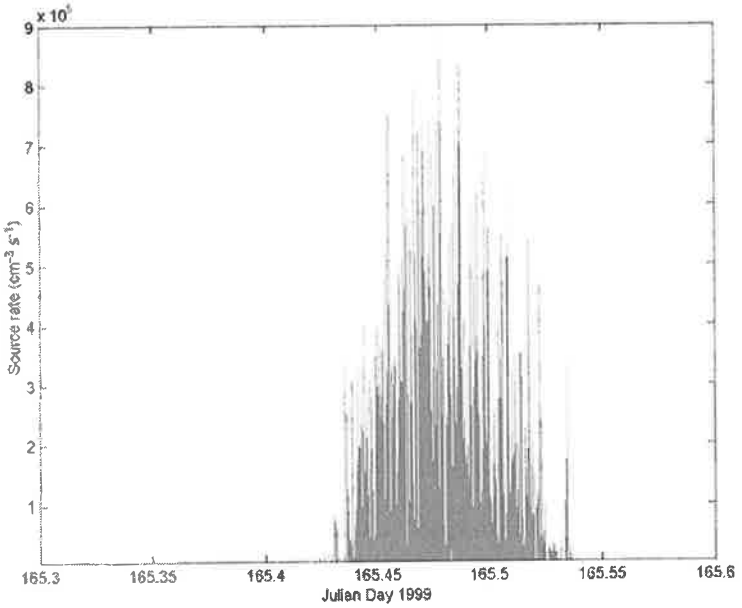

Figure 9. Formation rate of 3 nm particles during a type I event measured at 10 m.

less than 100 m upwind from the shore lab measurement points, the rate of change of nucleation mode particle concentration (i.e., the difference between 3 and 10 nm particle concentrations) per second can be regarded as the source rate of these sized particles. Furthermore, given the very short transit time of 10–20 s during type I events, coagulation loss is estimated to be of the order of 50% [*Pirjola et al.*, 2002] and consequently, the source rates of 3 nm particles can be regarded close to effective nucleation rates.

[37] The source rates of the type I event encountered on JD 165 are displayed in Figure 9 for the measurement nodes at 10 m. At the 10 m level, the source rates derived are typically between 100,000 and 200,000 cm^{-3} s^{-1}, with peak source rates of the order of 7×10^5 cm^{-3} s^{-1}. Given the known production region, and assuming that the critical embryo size for a new particles is of the order of 1 nm, initial condensation growth rates can be estimated for type I events from examination of the typical transit time between the production region and the measurement point at the shore laboratory. If the measurement point is 100 m from the tidal source region, then for a wind speed of 5 m s^{-1}, the transit time is 20 s. During this period, assuming that nucleation is almost instantaneous or there is already a dynamic reservoir of thermodynamically stable sulphur clusters (TSCs) [e.g., *Kulmala et al.*, 2000], which the biogenic gases can condense on, it takes 20 s for these TSCs to growth to 3 nm, resulting in a growth rate of 0.1 nm s^{-1}. The growth rate is more likely even higher than this, particularly during June when 10 nm particles were observed at the shore lab during type I events. From the appearance of 10 nm particles, a growth rate of 0.35 nm s^{-1} (1260 nm per hour) is estimated. These extraordinarily high growth rates are thought to result from the very intense biogenic sources right at the shoreline and at the start of the coastal plume but would not be expected to be sustained as the plume disperses. Other estimates of the growth rate in this environment have been made (that by *Dal Maso et al.* [2002], using a combination of an analytic tool and observed aerosol size distribution growth rates estimated growth rates as high as 180 nm per hour near the source region), while further from the source region, pseudo-Lagrangian airborne measurements of the evolution of the coastal plume offshore indicate that after the initial plume dispersal, growth rates of 14–15 nm per hour are encountered in the type III cases [*O'Dowd*, 2002] (no data were available for other case types).

3.7. Macroscale and Microscale Meteorological Conditions Associated With Particle Production Events

[38] Nucleation was observed under all air mass conditions, including Arctic, polar, temperate latitude, tropical maritime, and continental air masses. LIDAR measurements of boundary layer structure also indicated no apparent linkage with, or influence on, new particle production and are discussed in more detail by *Kunz et al.* [2002].

[39] Micrometeorological processes, however, promoting an increase in surface vapor flux, may also promote nucleation by providing additional water vapor, which increases the nucleation probability, along with possible nucleation precursors species. Similarly, increases in turbulent fluctuations (in temperature and humidity) can also significantly increase the probability of nucleation [*Easter and Peters*, 1994; *Nilsson and Kulmala*, 1998; *Pirjola et al.*, 2000]. In order to explore any relationship between micrometeorology and particle production, micrometeorological measurements were conducted at 3 m and ≈20 m (18 m in 1998, 22 m in 1999). Throughout the campaign, diurnal variations of water vapor fluxes were observed, with maximum values of 0.001–0.002 g kg^{-1} m s^{-1} around noon. Variations in drag coefficients and vertical variances of wind components were also especially related to wind direction, but also to speed, and thermal stability. During periods of onshore wind, the drag coefficients often exhibited some further enhancement during the occurrence of low tide. A detailed study of

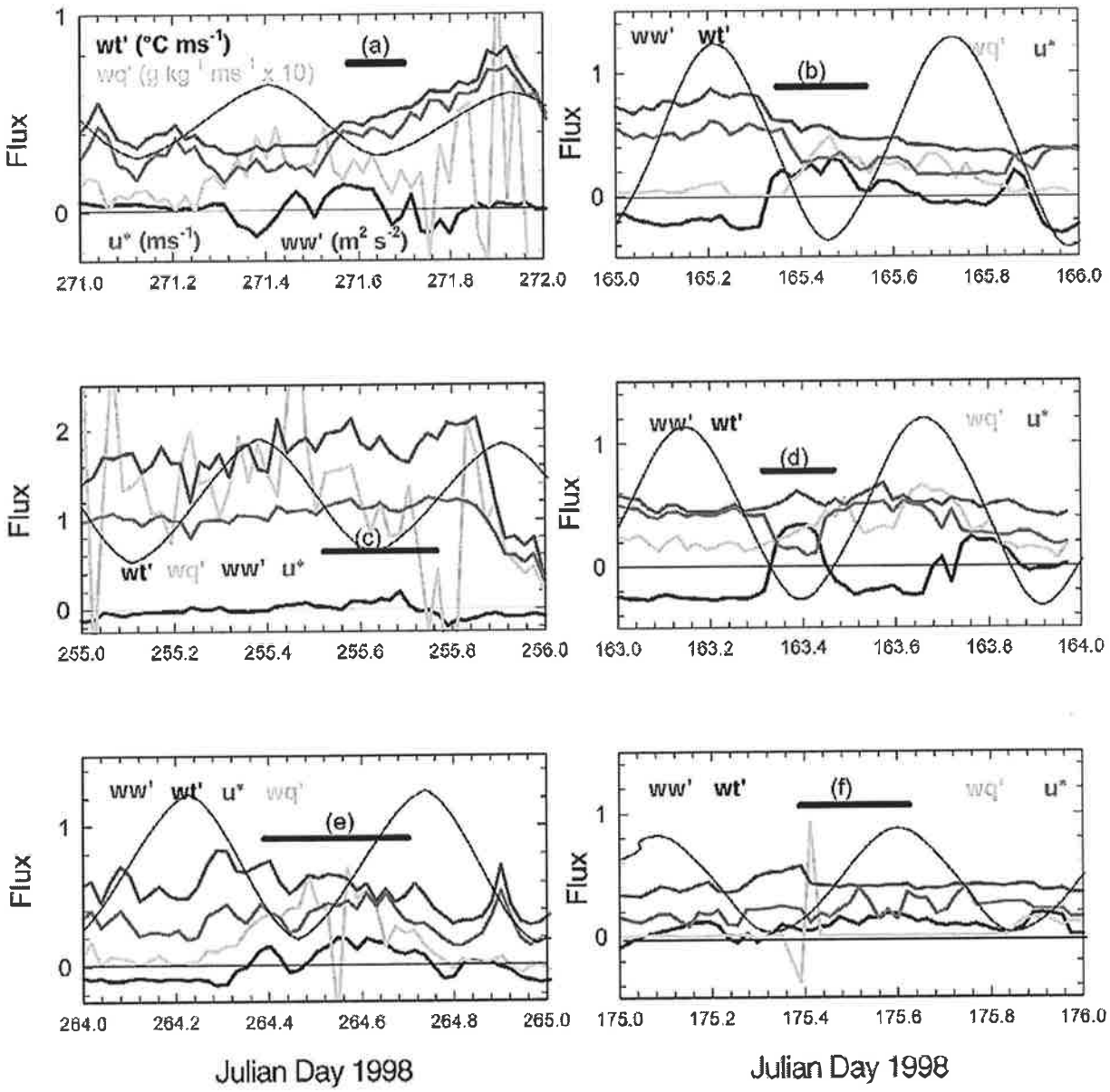

Figure 10. Micrometeorological parameters during event types encountered at Mace Head. Heat fluxes (*wt'*), water vapor fluxes (*wq'*), vertical wind variances (*ww'*), and *u**. (a) Type I event 1998. (b) Type I event 1999. (c) Type II event 1998. (d) Type II event 1999. (e) Type III event 1998. (f) Type III event 1999. The horizontal bar indicates the time of the nucleation event for each case.

micrometeorological characteristics at Mace Head during PARFORCE is given by *de Leeuw et al.* [2002].

[40] For the selected case studies corresponding to type I, II and III events, kinematic heat flux (°C m s^{-1}), and vapor flux (g kg^{-1} m s^{-1}) are displayed in Figure 10 along with vertical wind variances and friction velocity u^* (m s^{-1}). Tidal amplitude is shown for comparison. As already indicated above, vertical vapor flux was typically near zero throughout the night and increased generally to a maximum in the middle of the day or in the afternoon.

[41] Heat fluxes were much more variable, especially in 1999. The variations observed in 1998 had diurnal trends; often negative values were measured during the night and early morning, becoming positive during the day under the influence of solar irradiation. Minimum values were usually around -0.1°C m s^{-1}, and sometimes lower, daily maxima were usually between 0.1 and 0.2°C m s^{-1}. In 1999 the kinematic heat fluxes varied between -0.25 and $+0.25$°C m s^{-1}, often with a similar diurnal pattern as in 1998, but negative values were also observed during the afternoon, while positive values were just as often observed during night time.

[42] Vertical variances in the vertical wind speed component, *w'w'*, on these days was found to be within the range of 0.3–0.8 m^2 s^{-2} except for JD 255 where peak variances were found to approach 2 m^2 s^{-2} under the high wind

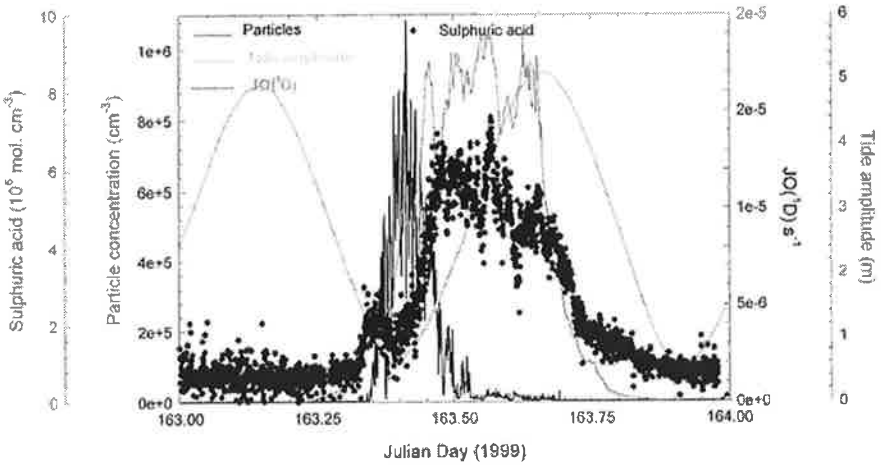

Figure 11. Total particle concentration ($d > 3$ nm), $JO(^1D)$, sulphuric acid and tidal amplitude during one coastal particle production event, June 1999.

conditions where mechanical mixing was strong. Apart from wind speed, wind direction influences the flow properties because of differences in terrain and thus surface roughness around the sample points. These effects also show up in u^* which was typically in the range of 0.2–0.7 m s^{-1} with enhanced values of >1 m s^{-1}, again occurring for the high wind case. While there are some trends visible indicating that, for onshore wind, turbulence is enhanced during low tide, the dominant influence on these variables appears to be more related to wind speed.

[43] Kinematic heat fluxes and humidity fluxes displayed the clearest relationship with nucleation events. In Figure 10 this is illustrated by the occurrences of low tide during daytime (see Figure 6 for the corresponding nucleation events). The most obvious trend between heat flux and low tide is seen for JDs 163 and 165. JD 165 shows both the increasing heat and humidity flux at low tide, while on JD 163 the humidity flux starts to increase during low tide and stays high until the end of the day. These trends are to be expected as during low tide, as the watermark declines, more land is exposed and the surface heats more readily as the water dries out (note that the measurements shown were made close to the high water mark, at 3 m above the surface). The positive heat and water vapor fluxes indicate that also other material such as biogenic gases emitted by the surface biota may be more readily transported away from the surface into the developing internal boundary layer [*de Leeuw et al.*, 2002].

[44] Furthermore, often during nucleation events, water vapor concentration variances were observed to peak, and in many cases, but less frequent, maxima in temperature variances were observed as well. The associated turbulent fluctuations in temperature and water vapor could promote nucleation as referred to above.

[45] In summary, during low tide events, turbulence is increased due to the enhanced surface roughness, as is the vapor and heat flux from the tidal zone. These factors likely promote the injection of biogenic precursor gases from the shore region along with promoting nucleation resulting from turbulent fluctuations. However, it has to be noted that while there is qualitative evidence for coherence between micrometeorological fluxes, turbulence and new particle formation, there is insufficient evidence to conclusively state that the enhanced vapor flux and turbulent variations initiate the necessary environmental conditions for significant nucleation to proceed.

4. Discussion

[46] The occurrence of coastal nucleation events appears independent of air mass origin and general meteorology; however, some micrometeorological influence was observed. The most obvious factor promoting particle production was the exposure of the coastal biota to the atmosphere under periods of solar irradiation. In terms of the most likely nucleating species, sulphuric acid is generally the first species implicated in ambient aerosol nucleation. Recent new ternary nucleation theory of sulphuric acid, water and ammonia suggest that significant nucleation could occur for sulphuric acid concentrations $>10^6$ molecules cm^{-3} and ammonia concentrations >100 ppt and also for sulphuric acid concentrations $>10^7$ molecules cm^{-3} and ammonia concentrations >10 ppt. For all cases, the combination of sulphuric acid and ammonia was always sufficient for nucleation of TSCs [*Kulmala et al.*, 2002]; however, no clear relationship was observed between sulphuric acid concentration and particle production [*Berresheim et al.*, 2002].

[47] Invariably, the peak in the concentration of sulphuric acid occurred at different times to that of the nucleation mode particles. This lack of coincidence between particle production and sulphuric acid concentration was shown in Figure 2 for JD 171 and is also illustrated in Figure 11 for one of the more intense events, occurring on JD 163. On JD 163, particle production, with peak concentrations >1,000,000 cm^{-3}, was observed at low tide (JD 163.3). Prior to the nucleation event, sulphuric acid concentrations were approaching 2.5–3 10^6 molecules cm^{-3}, and during the production period, the concentration decreased to $\approx 1 \times 10^6$ molecules cm^{-3}. After this reduction, the concentration continued to rise again, following the production rate of

$O(^1D)$, reaching a peak value of 6×10^6 molecules cm^{-3}. By this time, particle production had ceased and sulphuric acid concentration remained at $4-6 \times 10^6$ molecules cm^{-3} for a few hours. The reason for the apparent reduction in sulphuric acid vapor coinciding with the particle production event is not clear but could be due to homogeneous nucleation of thermodynamically stable clusters [*Kulmala et al.*, 2000, 2002] and/or condensation onto the preexisting aerosol.

[48] Due to the new particle production at these high concentrations, the aerosol condensation sink, using a sticking coefficient of 1 [*Dal Maso et al.*, 2002], increased by a factor of 3, thus suggesting that the sulphuric acid reduction may be due to enhanced condensation. From examination of the growth factors during this period, solubility was observed to increase during the latter stages of the production period and on through to the peak in sulphuric acid the afternoon. If nucleation on TSCs occurred, then the sulphuric acid concentration required to produce 10^5 particles cm^{-3} would be of the order 10^6 molecules cm^{-3}. If one extrapolates the sulphuric acid concentration between the concentrations observed before and after the event, the difference is 2×10^6 molecules cm^{-3}. Using this crude argument, ternary nucleation of TSCs is certainly feasible; however, there is insufficient sulphuric acid available to grow the TSCs into detectable particle sizes of >3 nm. Thus sulphuric acid may account for the nucleation of TSCs, but cannot explain the concentrations of detectable particles. While there is no correlation between particle concentrations and sulphuric acid concentration, there is always sufficient acid and ammonia to produce nucleation according to current theory [*Kulmala et al.*, 2002].

[49] The combination of particle occurrence invariably at low tide, under solar radiation, and with recently formed particles exhibiting a chemical composition other than sulphate, suggests that a low-solubility derivative of a biogenic gas emitted from the coastal algae and plants. Examination of biogenic VOC revealed no detectable concentration of aerosol-forming species emitted during tidal exposure [*Sartin et al.*, 2002]. Furthermore, no VOCs were detected from chamber emission experiments performed on various local seaweeds and algae [*Mäkelä et al*, 2002]. The seaweed experiments revealed, however, very strong emissions of halocarbon species and parallel measurements of short-lived alkyl iodides and their derivative IO, indicate significantly enhanced concentrations of these species during low tide [*Carpenter et al.*, 1999; *Alicke et al.*, 1999], thus pointing to a halocarbon derivative as a possible candidate for the primary condensing species.

[50] Single particle transmission electron microscopy measurements on samples during the second campaign [*Mäkelä et al.*, 2002] found evidence of both I and S in 8 nm particles but did not reveal any presence of Br or Cl. The presence of I in recently formed particles, and the reported link between elevated IO concentrations and tidal cycle suggest that the primary condensing species leading to coastal particle production is I. Recent laboratory studies on the chemical composition of aerosol particles, formed after photodissociation of CH_2I_2 in the presence of ozone, using online atmospheric pressure chemical ionization mass spectrometry indicate that iodine oxides can nucleate and readily condense to rapidly grow particles [*Hoffmann et al.*, 2001]. One possible pathway is through the photodissociation of CH_2I_2, releasing I, which reacts rapidly with ozone to produce IO. IO can then self-react to form OIO [*Cox et al.*, 1999], which can, in turn, self-react to produce the condensable vapor I_2O_4 [*Hoffmann et al.*, 2001]. Similarly, HI and HOI will readily condense, and since there is no Cl or Br found in these new particles, HI and HOI are likely to remain in the condensed phase [*McFiggans et al.*, 2000].

[51] Studies on the condensable vapor concentration required to produce these events indicate that the condensable vapor concentration required is of the order of 10^9-10^{10} molecules cm^{-3} with a source rate of 5×10^7 cm^{-3} s^{-1} [*Pirjola et al.*, 2000]. This is 2–3 order of magnitude higher that the calculated source rate of IO over the ocean phase [*McFiggans et al.*, 2000]; however, despite the reported concentrations of 6 ppt IO (1.6×10^8 molecules cm^{-3}) measured by long path DOAS during low tide at Mace Head, the actual IO concentrations are likely to be significantly higher than this. The configuration of the DOAS system at Mace Head required a transmission path across the bay to the northwest of Mace Head with a path length of 15 km. Crudely calculating the shore region coverage on both sides of the bay as 200 m path interference (corresponding to two tidal regions each of 100 m width), IO concentrations directly over the strong biogenic tidal regions could easily reach 2 orders of magnitude higher than the peak concentration recorded by the DOAS system. Additionally, over very short timescales off seconds, IO concentrations could reach values event higher than this. Thus it is feasible that the primary condensable species is an iodine oxide and that condensation is further accelerated by condensation of sulphuric acid, although considerable effort is required to more accurately elucidate, both from a theoretical and experimental perspective, the life cycle of iodine in the marine and coastal boundary layer, and is potential to nucleate new particles.

5. Conclusions

[52] Coastal nucleation events occur all year-round under all meteorological conditions. Their occurrence coincided with low tide and solar radiation suggesting a tidal-biological source of aerosol precursors and the requirement of photo-oxidation of precursor gases. Events could be characterized in terms of air mass trajectory and passage over tidal areas and in terms of clean marine air, modified-marine air and polluted air. Important precursor gas concentrations such as sulphuric acid and ammonia ranged from 2 to 12×10^6 molecules cm^{-3} and 10–2000 ppt, respectively. Peak particle concentrations could exceed 1,000,000 cm^{-3} and events could last from 2 to 8 hours in duration. Growth factor analysis of 8 nm particles indicated a low soluble mass fraction and indicated that sulphate is a minor chemical component of the nucleation mode particles in this environment. The estimated nucleation rates of new particles were of the order of 10^5 cm^{-3} s^{-1} with peak rates approaching at 10^6 cm^{-3} s^{-1}. Growth rates for nucleation mode particles at the coastal plume source are between 0.1 and 0.35 nm s^{-1}. This growth rate requires a vapor concentration of $>10^7$ molecules cm^{-3} and a source rate of 10^6 molecules cm^{-3} s^{-1}. Sulphuric acid concentrations were sufficient for significant particle nucleation, but insufficient to grow new particles into detectable sizes. An additional biogenic vapor, with low

solubility, is required to produce the observed particle concentrations. The most likely candidate is an iodine oxide produced from the photodissociation of CH_2I_2. Further effort is required to determine if sulphuric acid concentrations produce the required concentration of stable clusters (or TSC) or whether the production of particles at Mace Head can be explained solely by nucleation and condensation growth of an iodine oxide.

[53] **Acknowledgments.** This work was supported by the European Union under contract FNV4-CT97-0526 (PARFORCE).

References

Alicke, B., K. Hebestreit, J. Stutz, and U. Platt, Iodine oxide in the marine boundary layer, *Nature*, *397*, 572–573, 1999.

Berresheim, H., T. Elste, H. G. Tremmel, A. G. Allen, H.-C. Hansson, K. Rosman, M. Dal Maso, J. M. Mäkelä, M. Kulmala, and C. D. O'Dowd, Gas-aerosol relationships of H_2SO_4, MSA, and H: Observations in the coastal marine boundary layer at Mace Head, Ireland, *J. Geophys. Res.*, *107*, 10.1029/2000JD000229, in press, 2002.

Carpenter, L. J., and P. S. Liss, On the temperate sources of bromoform and other reactive organic bromine gases, *J. Geophys. Res.*, *105*, 20,539–20,548, 2000.

Carpenter, L. J., W. T. Sturges, S. A. Penkett, P. Liss, A. Alicke, K. Hebestreit, and U. Platt, Short-lived alkyl iodides and bromides at Mace Head, Ireland: Links to biogenic sources, *J. Geophys. Res.*, *104*, 1679–1689, 1999.

Clarke, A. D., et al., Particle nucleation in the tropical boundary layer and its coupling to marine sulfur sources, *Science*, *282*, 89–91, 1998.

Covert, D. S., V. N. Kapustin, T. S. Bates, and P. K. Quinn, New particle formation in the marine boundary layer, *J. Geophys. Res.*, *97*, 20,581–20,589, 1992.

Cox, R. A., W. J. Bloss, R. L. Jones, and D. M. Rowley, OIO and the atmospheric cycle of iodine, *Geophys. Res. Lett.*, *26*, 1857–1860, 1999.

Dal Maso, M., M. Kulmala, K. E. J. Lehtinen, J. M. Mäkelä, P. Aalto, and C. D. O'Dowd, Condensation and coagulation sinks and formation of nucleation mode particles in coastal and boreal forest boundary layers, *J. Geophys. Res.*, *107*, 10.1029/2001JD001053, in press, 2002.

de Leeuw, G., G. J. Kunz, G. Buzorius, and C. D. O'Dowd, Meteorological influences on coastal new particle formation, *J. Geophys. Res.*, *107*, 10.1029/2001JD001478, in press, 2002.

Easter, R. C., and L. K. Peters, Binary homogeneous nucleation: Temperature and relative humidity fluctuations, nonlinearity, and aspects of new particle production in the atmosphere, *J. Appl. Meteorol.*, *33*, 775–784, 1994.

Hämeri, K., C. D. O'Dowd, and C. Hoell, Measurements of new particle concentrations, source rates, and spatial scales during coastal nucleation events using condensation particle counters, *J. Geophys. Res.*, *107*, 10.1029/2001JD000411, in press, 2002.

Hoffmann, T., C. D. O'Dowd, and J. H. Seinfeld, Iodine oxide homogeneous nucleation: An explanation for coastal new particle production, *Geophys. Res., Lett.*, *27*, 1949–1952, 2001.

Korhonen, O., M. Kulmala, A. Laaksonen, Y. Viisanen, R. McGraw, and J. H. Seinfeld, Ternary nucleation of H_2SO_4, NH_3 and H_2O in the atmosphere, *J. Geophys. Res.*, *104*, 26,349–26,353, 1999.

Kulmala, M., L. Pirjola, and J. M. Mäkelä, Stable sulphate clusters as a source of new atmospheric particles, *Nature*, *404*, 66–69, 2000.

Kulmala, M., P. Korhonen, I. Napari, R. Jansson, H. Berresheim, and C. D. O'Dowd, Aerosol formation during PARFORCE: Ternary nucleation of H_2SO_4, NH_3 and H_2O, *J. Geophys. Res.*, *107*, 10.1029/2001JD000900, in press, 2002.

Kunz, G. J., G. de Leeuw, E. Becker, and C. D. O'Dowd, Lidar studies of the atmospheric boundary layer and locally generated sea spray aerosol plumes at Mace Head, *J. Geophys. Res.*, *107*, 10.1029/2001JD001240, in press, 2002.

Mäkelä, J. M., P. Aalto, V. Jokinen, A. Nissinen, S. Palmroth, T. Markkanen, K. Seitsonen, H. Lihavainen, and M. Kulmala, Observations of ultrafine aerosol particle formation and growth in boreal forest, *Geophys. Res. Lett.*, *24*, 1219–1222, 1997.

Mäkelä, J. M., T. Hoffmann, C. Holzke, M. Väkevä, T. Suni, T. Mattila, P. P. Aalto, U. Tapper, E. Kauppinen, and C. D. O'Dowd, Biogenic iodine emissions and identification of end-products in coastal ultrafine particles during nucleation bursts, *J. Geophys. Res.*, *107*, 10.1029/2001JD000580, in press, 2002.

McFiggans, G., J. M. C. Plane, B. J. Allan, L. J. Carpenter, H. Coe, and C. D. O'Dowd, A modeling study of iodine chemistry in the marine boundary layer, *J. Geophys. Res.*, *105*, 14,371–14,386, 2000.

Morgan, R., and A. Stroh, Measurements of gas-phase hydrogen peroxide and methyl hydroperoxide in the coastal environment during the PARFORCE project, *J. Geophys. Res.*, *107*, 10.1029/2000JD000257, in press, 2002.

Nilsson, E. D., and M. Kulmala, The potential for atmospheric mixing processes to enhance the binary nucleation rate, *J. Geophys. Res.*, *103*, 1381–1389, 1998.

O'Dowd, C. D., On the spatial extent and evolution of coastal aerosol plumes, *J. Geophys. Res.*, *107*, 10.1029/2001JD000422, in press, 2002.

O'Dowd, C. D., M. H. Smith, and S. G. Jennings, Submicron aerosol, radon, and soot carbon characteristics over the northeast Atlantic, *J. Geophys. Res.*, *98*, 1132–1136, 1993.

O'Dowd, C. D., J. A. Lowe, and M. H. Smith, Marine aerosol, sea-salt, and the marine sulphur cycle: A short review, *Atmos. Environ.*, *31*, 73–80, 1997a.

O'Dowd, C. D., B. Davison, J. A. Lowe, M. H. Smith, R. M. Harrison, and C. N. Hewitt, Biogenic sulphur emissions and inferred sulphate CCN concentrations in and around Antarctica, *J. Geophys. Res.*, *102*, 12,839–12,854, 1997b.

O'Dowd, C. D., M. Geever, M. K. Hill, S. G. Jennings, and M. H. Smith, New particle formation: Spatial scales and nucleation rates in the coastal environment, *Geophys. Res. Lett.*, *25*, 1661–1664, 1998.

O'Dowd, C. D., J. A. Lowe, M. H. Smith, and A. D. Kaye, The relative importance of sea-salt and nss-sulphate aerosol to the marine CCN population: An improved multi-component aerosol-droplet parameterisation, *Q. J. R. Meteorol. Soc.*, *125*, 1295–1313, 1999a.

O'Dowd, C. D., et al., On the photochemical production of new particles in the coastal boundary layer, *Geophys. Res. Lett.*, *26*, 1707–1710, 1999b.

O'Dowd, C. D., et al., A dedicated study of New Particle Formation and Fate in the Coastal Environment (PARFORCE): Overview of objectives and achievements, *J. Geophys. Res.*, *107*, doi:10.1029/2001000555, in press, 2002.

Pirjola, L., C. D. O'Dowd, I. M. Brooks, and M. Kulmala, Can new particle formation occur in the clean marine boundary layer?, *J. Geophys. Res.*, *105*, 26,531–26,546, 2000.

Pirjola, L., C. D. O'Dowd, and M. Kulmala, A model prediction of the yield of cloud condensation nuclei from coastal nucleation events, *J. Geophys. Res.*, *107*, 10.1029/2000JD000213, in press, 2002.

Sartin, H., C. J. Halsall, and C. N. Hewitt, Temporal patterns, sources, and sinks of C_8-C_{16} hydrocarbons in the atmosphere of Mace Head, Ireland, *J. Geophys. Res.*, *107*, 10.1029/2000JD000232, in press, 2002.

Schröder, F., and J. Ström, Aircraft measurements of submicrometer aerosol particles (>7 nm) in the mid-latitude free troposphere and troposphere region, *Atmos. Res.*, *44*, 333–357, 1997.

Väkevä, M., K. Hämeri, and P. Aalto, Hygroscopic properties of nucleation mode and Aitken mode particles during nucleation bursts and in background air on the west coast of Ireland, *J. Geophys. Res.*, *107*, 10.1029/2000JD000176, in press, 2002.

Vignati, E., G. de Leeuw, and R. Berkowicz, Modeling coastal aerosol transport and effects of surf-produced aerosols on processes in the marine atmospheric boundary layer, *J. Geophys. Res.*, *106*, 20,225–20,238, 2001.

Weber, R. J., et al., A study of new particle formation and growth involving biogenic trace gas species measured during ACE-1, *J. Geophys. Res.*, *103*, 16,385–16,396, 1998.

P. Aalto, K. Hämeri, M. Kulmala, J. Mäkelä, C. D. O'Dowd, and M. Väveka, University of Helsinki, Department of Physical Sciences, P.O. Box 64, FIN-00014 Helsinki, Finland. (pasi.p.aalto@helsinki.fi; kaarle.hameri@ttl.fi; Markku.kulmala@helsinki.fi; jyrki.makela@tut.fi; colin.odowd@cmas.demon.co.uk; minna.vakeva@helsinki.fi)

A. G. Allen and R. M. Harrison, Division of Environmental Health and Risk Management, School of Geography and Environmental Sciences, University of Birmingham, Edgbaston, Birmingham B15 2TT, UK. (a.g.allen@bham.ac.uk; r.m.harrison.ipe@bham.ac.uk)

E. Becker, Spectroscopic On-Line Analysis, Program Development, BP Chemicals Ltd., HRTC/DL10, Saltend Lane, Hedon HU12 8DS, UK. (beckere@bp.com)

H. Berresheim, Deutscher Wetterdienst, Meteorologisches Observatorium, Albin-Schwaiger-Weg 10, D-82383 Hohenpeissenberg, Germany. (harald.berresheim@dwd.de)

M. Geever, S. G. Jennings, C. Kleefeld, and M. Kulmala, Department of Physics, National University of Ireland, Galway, University Road, Galway, Ireland. (mgeever@eircom.net; gerard.jennings@nuigalway.ie; christoph.kleefeld@nuigalway.ie)

H.-C. Hansson, Institute for Applied Environmental Research, Air Pollution Laboratory, Stockholm University, Stockholm, Sweden. (HC@itm.su.se)

G. J. Kunz and D. de Leeuw, TNO Physics and Electronics Laboratory, P.O. Box 96864, N-2509 JG The Hague, Netherlands. (kunz@fel.tno.nl; deleeuw@fel.tno.nl)